Regular Paper

A Low-speed High-torque Permanent Magnet Synchronous Motor - Reducing Cogging Torque and Eddy Current Loss -

Taichi NAKAMURA[*1] (Stu. Mem.), Takafumi KOSEKI[*1] (Mem.) and Yasuaki AOYAMA[*2]

Various electric propulsion systems are used in the industrial field. Recently, research focused on permanent magnet synchronous motors (PMSMs) because of their several advantages. One advantage is high torque output; thus, this characteristic is suitable for application in a direct drive. The application to electric ships requires motors with the high torque at low speed. A transverse flux-type PMSM was investigated previously. However, this motor had two issues. One was high cogging torque. The other was eddy current loss in the disk. Thus, the authors propose a new design for a PMSM that reduces the cogging torque by employing a pole-core combination. In addition the material of the disk has been changed to reduce the eddy current loss. Finally, the characteristics of the newest prototype motor are explained.

Keywords: permanent magnet synchronous motor (PMSM), transverse flux machine (TFM), cogging torque, pole-core combination, eddy current loss.

(*Received: 10 October 2011, Revised: 17 March 2012, Accepted: 19 March 2012*)

1. Introduction

High-thrust electric motors are a significant component in many modern industrial and consumer applications. Recently, a permanent magnet synchronous motor (PMSM) has been attracting significant interest in the industrial field because a PMSM has advantages such as large output in spite of small size when compared with other traditional motors. This characteristic allows its application in direct-drive systems.

High-torque direct-drive motors can offer various advantages, such as reduced noise and vibration due to the absence of mechanical gear or transmission. Therefore, advantages in direct-drive machine technology are crucial for improving motor systems in applications such as electric cars, and one important industrial application for direct-drive motors is electric ships. Motors that drive ships require high torque at low speed; therefore, the transverse flux machine (TFM) is suitable to direct drives for electric ships. Previously, the transverse flux-type PMSM for ships was investigated [1, 2, 3]. However, there were two issues to be solved. One was high cogging torque that causes noise or vibration. The other was eddy current loss in the disk of the rotor.

The authors propose a new design to solve the above issues. In this paper, the configuration to reduce the cogging torque by employing a pole-core combination is described in details. Also, the material of the disk has been changed to reduce the eddy current loss. Finally, the specification of the newest prototype motor is described in comparison with the previous prototype motor.

Correspondence: T. NAKAMURA Department of Electrical Engineering and Information Systems, Graduate School of Engineering, The University of Tokyo, 7-3-1, Hongo, Bunkyo- ku, Tokyo, 113-8656, Japan
e-mail: t_nakamura@koseki.t.u- tokyo.ac.jp
[*1] The University of Tokyo, [*2] Hitachi Research Laboratory

2. C core-Type Transverse Flux-Type PMSM

2.1 Transverse Flux-Type PMSM

The TFM, introduced by Weh, Hoffmann, and Landrath [4] is the most recent major evolution in PMSMs for direct drives. Magnetic flux flows perpendicular to the direction of rotation in the TFM. Hence, a TFM takes advantage of an increase of torque production without a trade-off between electrical and magnetic loading as in the case of radial or axial flux machines. The configuration of a TFM is shown in Fig. 1. Also Hitachi's Tunnel Actuator (TA) for linear drive applications can produce high thrust with a similar flux path configuration [5].

2.2 C Core-Type Transverse Flux Motor

The C core-type transverse flux motor based on the concept of the TA structure in Fig. 2 was investigated through the use of electric ships [1, 2, 3]. The remarkable characteristic of the motor was a combination of 38 magnets and 18 cores with an expectation of high torque [3]. However, there were two issues that needed to be solved. One was high cogging torque, and the other was eddy current loss in the disk.

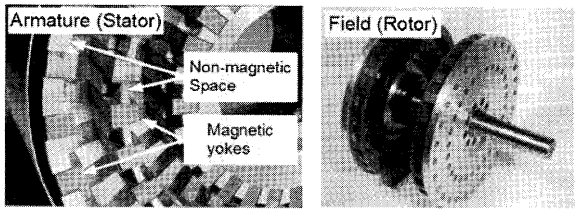

Fig. 1. Original transverse flux machine by Weh [4].

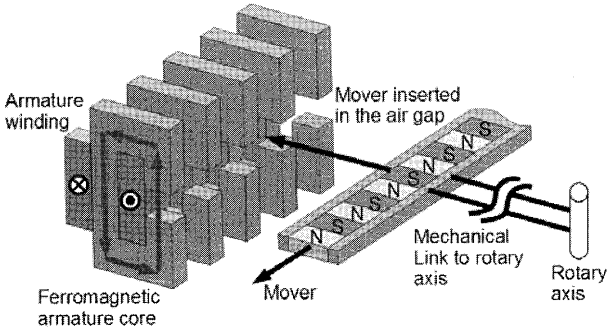

Fig. 2. Flux path through the C core and the magnet.

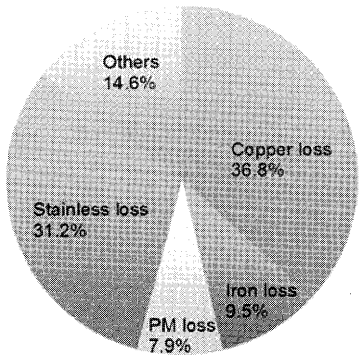

Fig. 3. Empirical losses under no load operation [3].

The cogging torque is often observed in PMSMs. It causes excessive noise and harmful vibration to the machine. The skewing method was employed to reduce the cogging torque in the previous prototype motor (2nd prototype motor). However, high cogging torque was generated, and the motor could not rotate smoothly. It was 3.5 Nm by the finite element method, which was 1/9 of the rated torque. For this reason, another method to reduce the cogging torque must be discussed.

The temperature of the rotor disk, which was made from stainless steel, increased through the continuous drive for 30 min. The authors suspected that this was due to the eddy current loss in the support material, i.e., stainless steel. Fig. 3 shows the measurement result of each loss under no load, when the driving frequency was 35 Hz. It is found that the eddy current loss in the disk accounts for 30 % of the total loss under no load. The electrical resistivity of the stainless steel used in the rotor is 7.2×10^{-7} Ωm. Hence, the rotor should be made from a material that has higher electrical resistivity with high strength such as a fiber-reinforced plastic (FRP) to reduce the eddy current.

3. Design of the New C Core-Type Transverse Flux Motor

3.1 Cogging Torque with a Pole-Slot Combination

The 2nd prototype motor could not rotate smoothly because of a high cogging torque. The cogging torque causes excessive noise and harmful vibration to the machine; hence, a method to reduce the cogging torque must be discussed. The authors studied the pole-slot combination. The bigger the least multiple of poles and the slot numbers are, the less the cogging torque is [6]. Therefore, this method is often employed on a PMSM.

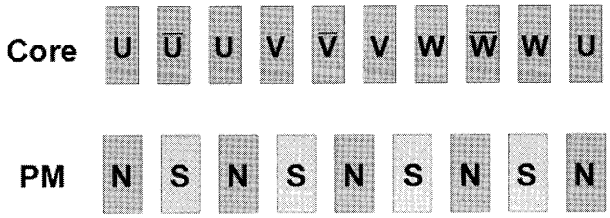

Fig. 4. Linear model of 8-pole, 9-slot combination.

3.1.1 Configuration of 8-pole, 9-core combination

Fig. 4 shows the configuration of the 8-pole, 9-slot combination.

Each phase is ordered in the following sequence;

U, Ū, U, V, V̄, V, W, W̄, W, and U.

Therefore, the concentrated windings must be employed on the slots in the 8-pole, 9-slot combination.

In the design of PMSMs, the value of the magnetomotive force by the armature is important to obtain high torque. To avoid the spatial constraint of the winding turns, windings were wound around three cores of the phases, which were the same as in the 2nd prototype motor. However, each winding must be concentrated in the 8-pole 9-slot combination. The authors propose a novel configuration in which windings are wound around three cores, keeping the same configuration of magnets and cores in the 8-pole, 9-core combination.

3.1.2 Proposed magnet core combination

The number of the U phase is different from the number of the Ū phase in the 8-pole, 9-core combination. Therefore, a pair of the 8-pole, 9-slot configuration is considered to make up the number of each phase, as shown in Fig. 5. All cores are labeled to be distinguishable, as shown in Fig. 5. Each core position was measured in electrical degrees starting from the nearest N-pole magnet and was discussed in the context of keeping the original combination of 8 magnets and 9 cores, as shown in Fig. 4. Table 1 shows each core position from the nearest N-pole magnet.

The authors determined that the number of magnets is 50 to achieve high torque. Each core is ordered so that windings are wound around the same three-phase cores. When the U1 core position is the origin, each core must be arranged to keep the distance from the nearest N-pole magnet listed in Table 1. Fig. 6 shows the concept of the new proposed configuration. Table 2 shows the position of each core in the proposed 50-pole, 18-core combination measured in electrical degrees.

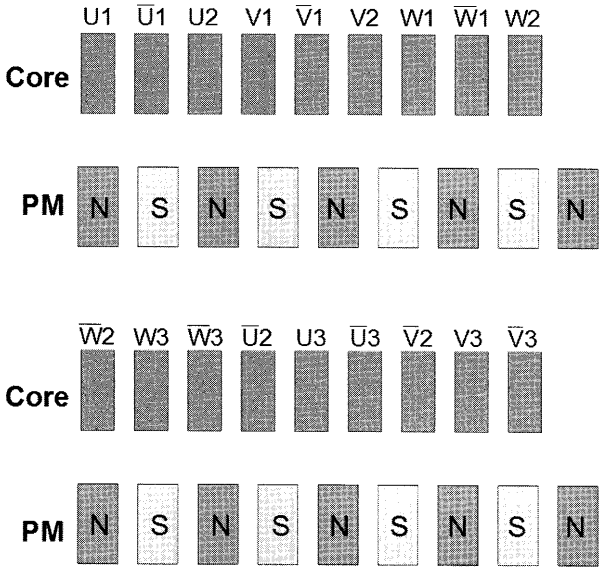

Fig. 5. A pair of 8-pole, 9-core combination.

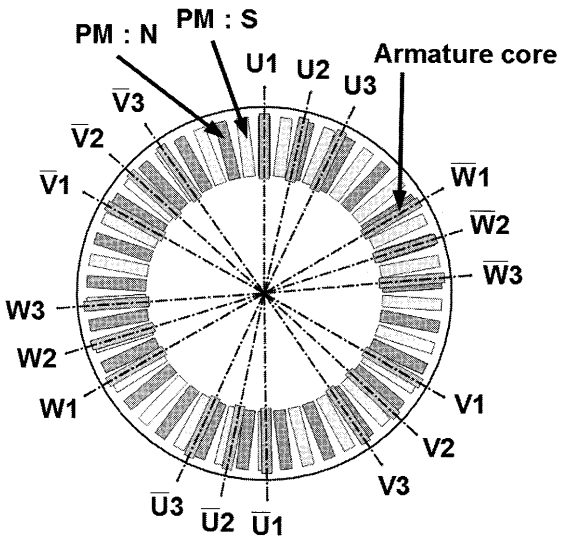

Fig. 6. Proposed magnet-core combination.

Table 1 Each core position from the nearest N-pole magnet.

Core name	Distance from the nearest N-pole magnet
U1	0
U2	- 2π / 9
U3	- 4π / 9
V1	6π / 9
V2	4π / 9
V3	2π / 9
W1	- 6π / 9
W2	- 8π / 9
W3	8π / 9
$\bar{U}$1	8π / 9
$\bar{U}$2	6π / 9
$\bar{U}$3	4π / 9
$\bar{V}$1	- 4π / 9
$\bar{V}$2	- 6π / 9
$\bar{V}$3	- 8π / 9
$\bar{W}$1	2π / 9
$\bar{W}$2	0
$\bar{W}$3	- 2π / 9

Table 2 Each core position in the proposed Configuration.

Core name	Position measured in electrical degrees	Distance from the nearest N-pole magnet
U1	0	0
U2	16π / 9	- 2π / 9
U3	32π / 9	- 4π / 9
$\bar{W}$1	74π / 9	2π / 9
$\bar{W}$2	90π / 9	0
$\bar{W}$3	106π / 9	- 2π / 9
V1	150π / 9	6π / 9
V2	166π / 9	4π / 9
V3	182π / 9	2π / 9
$\bar{U}$1	224π / 9	8π / 9
$\bar{U}$2	240π / 9	6π / 9
$\bar{U}$3	256π / 9	4π / 9
W1	300π / 9	- 6π / 9
W2	316π / 9	- 8π / 9
W3	332π / 9	8π / 9
$\bar{V}$1	374π / 9	- 4π / 9
$\bar{V}$2	390π / 9	- 6π / 9
$\bar{V}$3	406π / 9	- 8π / 9

3.2 Core Design and New Material of the Disk

3.2.1 Core Design

When the windings are wound around the three same phase cores as the configuration of the 2nd prototype motor [3], the flux linkage of the air gap between the core teeth decreases because the magnetic circuit is generated around the space. Hence, windings are placed close to the air gap so that the effective flux linkage can be maximized. Therefore, the new armature core is shown in Fig. 7.

This design has another advantage, which is effectively a skewed relationship between the magnet and the core teeth. That characteristic is expected to contribute to a decreasing the cogging torque.

3.2.2 New Material for the Disk of theRotor

The eddy current loss in the rotor disk is a serious issue, as already mentioned in Section 2. Hence, carbon fiber-reinforced plastic (CFRP) was used as the material of the rotary disk. The electrical resistivity of the CFRP is approximately 0.1 Ωm, which is 10^5 times larger than that of stainless steel. Therefore, the eddy current can not flow and the eddy current loss in the disk is drastically suppressed although the material and machining of the CFRP are rather expensive.

3.3 Analysis of the Proposed Model Using FEM

3.3.1 Design with the Low Cogging Torque

When the 8-pole, 9-core configuration is employed on a PMSM to reduce the cogging torque, it is precisely important to adjust the size of the magnet, the width of the core teeth, and the radius of rotation. The authors have decided the size of the magnet and the width of the core tooth in advance as shown in Table 3, and adjusted the radius of rotation. The thickness of the CFRP must be greater than 1.5 mm to retain the strength. Hence, the authors analyzed the cogging torque using FEM with this constraint when the range of the radius of rotation was from 75 mm to 90 mm using the model, as shown in Fig. 8. The maximum value of the cogging torque in each case is shown in Fig. 9.

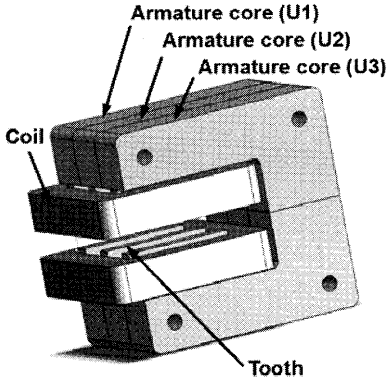

Fig. 7. Design of an armature core in the proposed model.

Table 3 Magnet size and tooth width.

Magnet size	6 mm × 30 mm × 5 mm
Tooth width	5 mm

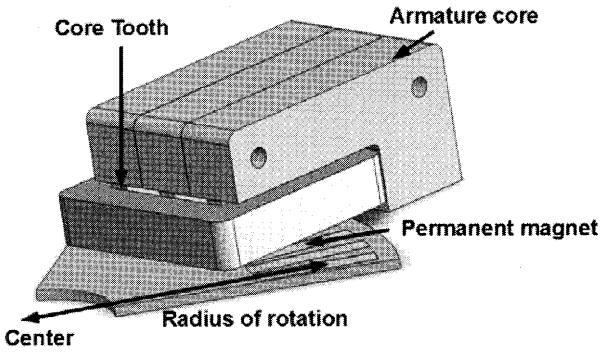

Fig. 8. Proposed model for FEM analysis.

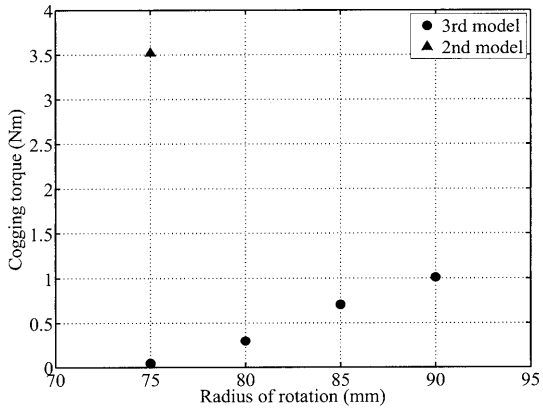

Fig. 9. Numerical result of the maximum cogging torque in each radius of rotation.

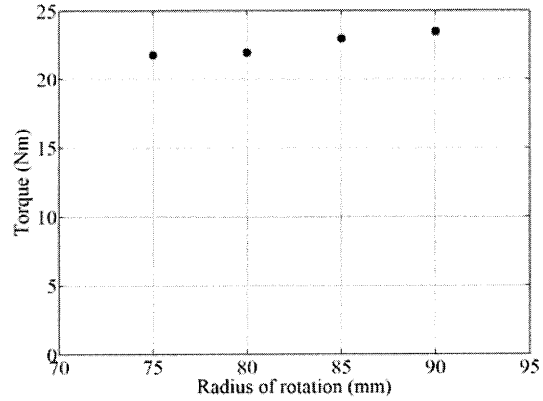

Fig. 10. Numerical result of static torque in each radius of rotation.

Table 4 Specification of the proposed model.

Specification	Proposed model	
Winding (turns)	400	
Rated current (A)	2.0	
Winding resistance (Ω)	4.4	
Self-inductance (H)	0.049	
	Proposed	2nd motor
Torque (Nm)	21.3	33.7
Torque density (Nm / L)	5.7	5.5
Maximum cogging torque (Nm)	0.04	3.5
Power factor	0.75	0.58
Drive frequency (Hz)	35	35

The maximum value of the cogging torque is effectively suppressed to only 0.04 Nm when the radius of rotation is 75 mm. Consequently, the cogging torque in the proposed model is approximately 80 times smaller than that in the 2nd prototype motor. Therefore, the new design is successful in suppressing the cogging torque.

3.3.2 Static Torque Analysis

It was decided that the winding turns should have 400 turns per core unit, and the result of the maximum torque in each case is shown in Fig. 10.

The maximum torque in each case is nearly the same. On the other hand, the maximum cogging torque is only 0.04 Nm when the radius of rotation is 75 mm. The authors decided that the radius of rotation was 75 mm after considering both these results and the process limitation of the CFRP to retain its strength.

3.4 Specification of the Proposed Model by FEM

The specification of the proposed model is calculated when the d-axis current is zero and the q-axis current is 2.0 A. Table 4 shows both the specification of the proposed model and the 2nd prototype motor.

The cogging torque is expected to decrease significantly in the proposed model. In addition, the power factor is improved when compared to the 2nd prototype motor when the d-axis current is 0, because the windings are wound near the air gap. On the other hand, the output torque is reduced. However, the characteristics of the torque density are almost the same. This result means that the torque density does not decrease drastically using the pole-core combination. The downsized core design also contributes to retain the torque density.

4. Machine Parameter Characterization

4.1 Newest Prototype Motor with the Low Cogging Torque

The newest prototype motor (3rd prototype motor) based on the proposed design was manufactured as shown in Fig. 11. However, the winding turns were

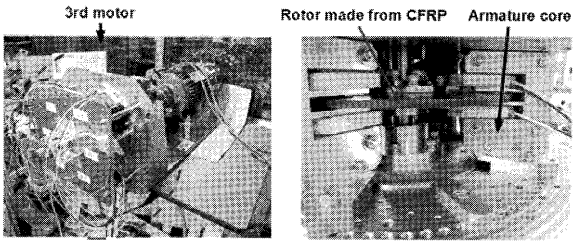

Fig. 11. The newest prototype motor.

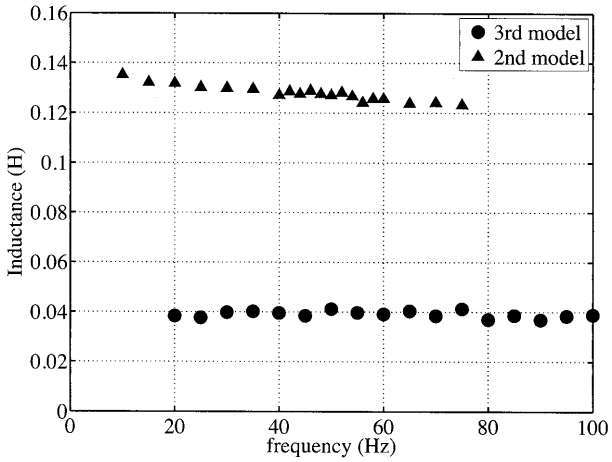

Fig. 12. Self-inductance measurement.

altered to 334 turns per core unit because of space constraints. The rotation of the motor in the open circuit was as smooth as expected. This result confirms the successful suppression of the cogging torque in the proposed magnet core combination.

4.2 Experimental Results

4.2.1 Armature Resistivity and Self-Inductance Measurement Results

The armature resistance per core unit was measured using a DC-voltage drop test. The armature resistance per core unit was 4.03 Ω. The self-inductance per core unit was measured using an AC-voltage source. The experimental result is shown in Fig. 12.

The frequency dependence of the self-inductance is plotted in Fig. 12. The self-inductance decreases with frequency in the 2nd prototype motor because the eddy current, which causes the effect of a magnetic screen, is generated in the disk made from stainless steel. On the other hand, self-inductance in the 3rd prototype motor remains constant as frequency increases. The authors suspect that the flow of the eddy current is prevented using the CFRP from the experimental result.

4.2.2 Specification of the 3rd Prototype motor

The authors estimated the specification using the experimental results when the d-axis current is zero and the q-axis current is 2.0 A.

Table 5 Specification based on empirical data in the 3rd prototype motor.

Specification	3rd motor	2nd motor
Armature resistivity (Ω)	4.0	5.1
Ampere-turns per core unit (AT)	668	668
Self-inductance (H)	0.04	0.137
Induced internal voltage (V)	24.7	32.5
Torque (Nm)	16.9	28.1
Torque density (Nm / L)	4.5	4.6
Power factor	0.78	0.58
Drive frequency (Hz)	35	35

The estimated specification of the 3rd prototype motor and the specification of the 2nd prototype motor under the same ampere turns are shown in Table 5.

The torque density is almost the same as the 2nd prototype motor regardless of reducing the cogging torque successfully in the 3rd prototype motor. However the torque density is only 40 % of commercial motors with similar size. This is because the space-utility factor is low in the 3rd prototype motor. Therefore, the space utility-factor should be maximized for larger output torque.

5. Conclusion

A new design of a disk rotor-type transverse flux machine to reduce the cogging torque and the eddy current loss has been described in this paper.

It is significant that the cogging torque is reduced retaining the torque density by applying the pole-core combination such as the 8-pole, 9-core combination. A considerable decrease of the cogging torque to only 0.04 Nm was achieved in the proposed motor. In addition, the result of the frequency dependency of the self-inductance measurement shows that the eddy current loss decreases by employing the CFRP to the disk of the proposed motor. Windings should be wound around the core teeth as close to the air gap as possible to increase the flux linkage of the air gap. This method contributes to an improvement of the power factor.

As the next work, the authors are controlling the 3rd prototype motor when the d-axis current is zero and verify the specification of the motor. The quantitative evaluation of each loss, including the eddy current loss in the disk, can be also verified experimentally.

In spite of such improvements, higher torque density was not achieved in the 3rd prototype motor when compared to existing industrial high torque products such as axial flux motors. Therefore, a substantially better space utility shall be investigated in the next design. The authors will design a new model after carefully considering the effective utilization of space and the pole-core combination.

Acknowledgment

We would like to thank MT-Drive (MTD) and the Japan Society for the Promotion of Science (JSPS) for their friendly support to this research. We would like to thank Enago (www.enago.jp) for the English language review, too.

References

[1] G. Patterson, T. Koseki, Y. Aoyama and K. Sako, "Simple modeling and prototype experiments for a new high-thrust, low-speed permanent magnet disk motor," *Proc. 12th Int. Conf. Electrical Machines and Sys.*, Tokyo, Jpn., 2009

[2] K. Sato, J. S. Shin, T. Koseki and Y. Aoyama, "Basic experiments for high-torque, low-speed permanent magnet synchronous motor and a technique for reducing cogging torque," *Int. Conf. Electrical Machines*, Roma, Italy, 2010.

[3] K. Sato, T. Koseki, and Y. Aoyama, "Design and verification of permanent magnet synchronous motor for high torque drive at low speed," RM-10-147 (In Japanese reviewing), 2010.

[4] H. Weh, H. Hoffman and J. Landrath, "New permanent magnet excited synchronous machine with high efficiency at low speeds," *Proc. Int. Conf. Electrical Machines*, 1988.

[5] H. J. Kim, J. Nakatsugawa, K. Sakai and H. Shibata, "High-acceleration linear motor, "Tunnel actuator"," *J. Magn. Soc. Jpn.*, Vol. 29, No. 3, pp. 199-204, 2005.

[6] T. Sun, J. M. Kim, G. H. Lee, J. P. Hong and M. R. Choi, "Effect of pole and slot combination on noise and vibration in permanent magnet synchronous motor," *IEEE Trans. Magn.*, Vol. 47, No. 5, May, 2011.